

See discussions, stats, and author profiles for this publication at: <https://www.researchgate.net/publication/231647302>

# Acidic Strengths of Brønsted and Lewis Acid Sites in Solid Acids Scaled by $^{31}\text{P}$ NMR Chemical Shifts of Adsorbed Trimethylphosphine

ARTICLE in THE JOURNAL OF PHYSICAL CHEMISTRY C · MARCH 2011

Impact Factor: 4.77 · DOI: 10.1021/jp200811b

CITATIONS

21

READS

171

8 AUTHORS, INCLUDING:



Zhiwu Yu

Wuhan National High Magnetic Field Center

18 PUBLICATIONS 252 CITATIONS

SEE PROFILE



Anmin Zheng

Chinese Academy of Sciences

104 PUBLICATIONS 1,634 CITATIONS

SEE PROFILE



Shing-Jong Huang

National Taiwan University

75 PUBLICATIONS 1,199 CITATIONS

SEE PROFILE



Shang-Bin Liu

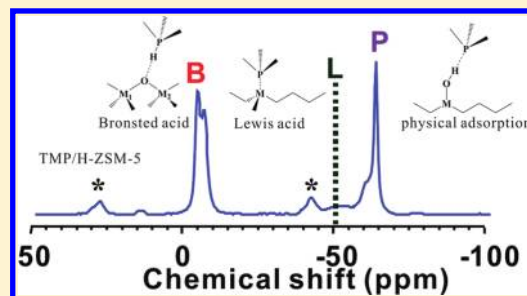
Academia Sinica

163 PUBLICATIONS 3,564 CITATIONS

SEE PROFILE

Acidic Strengths of Brønsted and Lewis Acid Sites in Solid Acids Scaled by  $^{31}\text{P}$  NMR Chemical Shifts of Adsorbed TrimethylphosphineYueying Chu,<sup>†</sup> Zhiwu Yu,<sup>†</sup> Anmin Zheng,<sup>\*,†</sup> Hanjun Fang,<sup>†</sup> Hailu Zhang,<sup>‡</sup> Shing-Jong Huang,<sup>§</sup> Shang-Bin Liu,<sup>\*,||,⊥</sup> and Feng Deng<sup>\*,†</sup><sup>†</sup>State Key Laboratory of Magnetic Resonance and Atomic and Molecular Physics, Wuhan Center for Magnetic Resonance, Wuhan Institute of Physics and Mathematics, The Chinese Academy of Sciences, Wuhan 430071, China<sup>‡</sup>Suzhou Institute of Nano-tech and Nano-bionics, The Chinese Academy of Sciences, Suzhou 215125, China<sup>§</sup>Department of Chemistry, National Taiwan University, Taipei 10617, Taiwan<sup>||</sup>Institute of Atomic and Molecular Sciences, Academia Sinica, P.O. Box 23-166, Taipei 10617, Taiwan<sup>⊥</sup>Department of Chemistry, National Taiwan Normal University, Taipei 11677, Taiwan

**ABSTRACT:** The validity of using  $^{31}\text{P}$  NMR of adsorbed trimethylphosphine (TMP) as a probe molecule for discerning the types (Brønsted vs Lewis) and strengths of acid sites in solid acid catalysts have been studied by density functional theory (DFT) calculations. Brønsted acid sites with varied acidic strengths covering from weak, strong, to superacid, mimicked by 8T zeolite cluster models having different Si–H bond lengths and hence proton affinities, were examined together with Lewis acid systems having different metallic centers, e.g.,  $\text{BCl}_n\text{F}_{3-n}$  ( $n = 0-3$ ),  $\text{AlCl}_n\text{F}_{3-n}$  ( $n = 0-3$ ), and  $\text{TiCl}_n\text{F}_{4-n}$  ( $n = 0-4$ ) and their mixed halides. The theoretical  $^{31}\text{P}$  chemical shifts predicted for the hydrogen-bonded  $\text{TMP}\cdots\text{H}$  complex and the  $\text{TMPH}^+$  adducts were  $-61 \pm 1$  and  $-3 \pm 1$  ppm, respectively, in good agreement with the experimental data. For the  $\text{TMP}$ –Lewis acid complex, a linear correlation between the calculated  $^{31}\text{P}$  chemical shifts and corresponding binding energies was observed for the B-, Al-, and Ti-containing Lewis acids, respectively, indicating the feasibility of using the  $^{31}\text{P}$  chemical shift of adsorbed TMP as a scale for Lewis acidic strength.



## 1. INTRODUCTION

An extensive experimental study on acid properties and the corresponding reaction mechanisms have been made for various solid acid catalysts.<sup>1</sup> The most critical issues involved during such acidity characterization are the precise determination of the types (Brønsted vs Lewis), strengths, concentrations, and locations of acid sites.<sup>2</sup> In particular, a variety of different solid-state nuclear magnetic resonance (NMR) techniques have been developed to investigate the surface acidities of solid acid catalysts utilizing probe molecules enriched with assorted nuclei such as  $^1\text{H}$ ,  $^{13}\text{C}$ ,  $^{31}\text{P}$ , etc. For example, by combining experimental NMR measurements with density functional theory (DFT) calculations, respective correlations of  $^{13}\text{C}$ ,  $^{31}\text{P}$ , and  $^1\text{H}$  chemical shifts with corresponding proton affinity (PA) of Brønsted acidities for 2- $^{13}\text{C}$ -acetone,<sup>3,4</sup> trimethylphosphine (TMP),<sup>5-14</sup> or trialkylphosphine oxides ( $\text{R}_3\text{PO}$ )<sup>2,15-20</sup> and pyridine- $d_6$ <sup>21</sup> have been successfully obtained. While such correlations between NMR chemical shifts ( $\delta$ s) and PAs have been shown useful as scales for quantitative interpretations of Brønsted acid strengths in various solid acid catalysts,<sup>19,20</sup> to the best of our knowledge, similar correlations between the observed  $\delta$ s of the probe nucleus species and strengths of Lewis acidities have rarely been explored.

Pioneered by Lunsford and co-workers,<sup>5,6</sup> TMP was first adopted as a probe molecule to characterize the acidity of H-form

faujasite-type zeolites based on the observed  $^{31}\text{P}$  NMR chemical shifts ( $\delta^{31}\text{P}$ s). Thereafter, the technique has been widely utilized for acidity characterization of various solid acid catalysts.<sup>5-14</sup> It has been shown that upon adsorbing a TMP molecule onto a Brønsted acid proton the subsequent formation of a  $\text{TMPH}^+$  ionic complex (Scheme 1a) tends to give rise to a  $^{31}\text{P}$  resonance with  $\delta^{31}\text{P}$  ranging from ca. -3 to -5 ppm, whereas TMP molecules bound to Lewis acid sites (Scheme 1c) normally result in  $^{31}\text{P}$  resonances with  $\delta^{31}\text{P}$ s in the range of ca. -20~-60 ppm (see Table 1). In other words, Brønsted (proton donor) and Lewis acid (electron acceptor) sites presenting in a solid acid catalyst can readily be distinguished using solid-state  $^{31}\text{P}$  magic-angle-spinning (MAS) NMR of adsorbed TMP.

In principle, the formation of a  $\text{TMP}$ –Lewis acid complex may be realized by the coordination of the P atom (on the TMP probe molecule) at a Lewis acid center (such as metal atoms; see Scheme 1c). For instance, a series of  $^{31}\text{P}$  NMR signals with  $\delta^{31}\text{P}$ s ranging from -32 to -58 ppm were observed for TMP adsorbed on severely calcined H-Y zeolites, indicating the presence of different Lewis acid centers in addition to the Brønsted acid site

Received: January 26, 2011

Revised: March 13, 2011

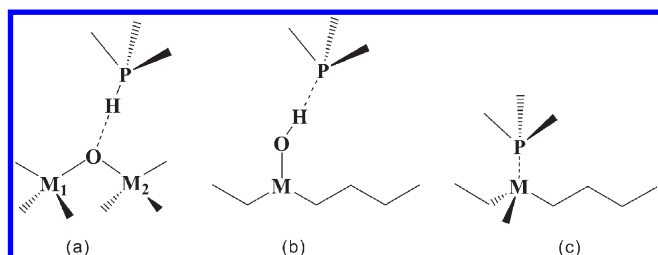
Published: March 28, 2011

(at ca.  $-4.2$  ppm; see Table 1).<sup>6,11</sup> Likewise, when the TMP probe molecule is adsorbed on the extra-framework Al species of a H-beta zeolite, two different Lewis acid sites with  $\delta^{31}\text{P}$ s at  $-32$  and  $-47$  ppm were identified.<sup>22</sup> On the basis of DFT calculations at the B3LYP/6-31G(d, p) level, the  $^{31}\text{P}$  resonance at  $-32$  ppm has been attributed to the presence of the extra-lattice oxo- $\text{AlOH}^{2+}$  species, whereas the peak at  $-47$  ppm was ascribed due to a synergic effect arising from the 3-fold coordinated lattice-Al species and the extra-lattice oxo-Al species interacting with the Brønsted acid sites (such as  $\text{Al}(\text{OH})_3$ ,  $\text{AlO}^+$ , and  $\text{Al}(\text{OH})_2^+$ ).<sup>22</sup> For Lewis acidity originating from a boron center, e.g.,  $\text{BF}_3$  supported on  $\gamma\text{-Al}_2\text{O}_3$ , a single  $^{31}\text{P}$  peak with  $\delta^{31}\text{P}$  at  $-26$  ppm was observed for the adsorbed TMP.<sup>23</sup> The Lewis acid sites on the surfaces of the supported  $\text{BF}_3/\gamma\text{-Al}_2\text{O}_3$  catalyst were found unassociated with the Al atoms, as evidenced by the negligible  $^{27}\text{Al}/^{31}\text{P}$  TRAPDOR effect observed for the  $^{31}\text{P}$  resonance. Further study by DFT calculation confirmed that the  $^{31}\text{P}$  resonance arises from TMP adsorbed on boron-containing Lewis acid sites, such as 3-fold coordinated boron species.<sup>23</sup> A similar technique has been adopted for characterization of Lewis acid sites in solid acid systems containing Zr, Ti, and Sn centers, leading to  $\delta^{31}\text{P}$ s of adsorbed TMP in the range  $-24$  to  $-50$  ppm (Table 1).<sup>14,24–28</sup> For example, two types of Lewis acidic

sites with  $\delta^{31}\text{P}$ s at  $-34.2$  and  $-32.0$  ppm were observed for TMP adsorbed on titanosilicate (TS) zeolites (Table 1), which have been assigned due to the presence of  $\text{Ti}(\text{OSiO}_3)_4$  and  $(\text{OSiO}_3)_3\text{Ti}(\text{OH})$  species, respectively.<sup>27,28</sup>

Despite the intensive experimental NMR studies on various solid acid catalyst systems using TMP as the probe molecule, a quantitative interpretation of Lewis acid strength remains a challenging task. In view of the fact that the linear correlation between the observed  $\delta^{31}\text{P}$  of adsorbed  $\text{R}_3\text{PO}$  with PA has been successfully used as a scale for quantitative interpretation of Brønsted acidic strength in various solid acid catalysts,<sup>19,20</sup> the wide range of  $\delta^{31}\text{P}$  observed for the TMP–Lewis acid complexes in Table 1 for various solid acids provides an opportunity to scale the acidic strengths of Lewis acid sites. The objective of this study therefore aims to authenticate such a scale for Lewis acidic strength by means of  $\delta^{31}\text{P}$ s estimated from the TMP–Lewis acid complexes by DFT quantum chemical calculations. As illustrated by a variety of metal-containing solid acid systems, for example, those possessing B-, Al-, and Ti-containing acid centers, the adsorption structures and the corresponding  $\delta^{31}\text{P}$ s of TMP adsorbed on various Lewis centers were systematically investigated. Accordingly, the correlations between calculated  $\delta^{31}\text{P}$ s and strengths of Lewis acid sites in various solid acid catalyst systems will be examined.

**Scheme 1. Three Scenarios of Adsorbed Trimethylphosphine (TMP): (a) Chemisorbed on Brønsted Acid Sites (i.e., Formation of  $\text{TMPH}^+$  Ionic Complexes), (b) Physisorbed on Hydroxyls (Hydrogen Bonding Interactions), and (c) Chemisorbed on Lewis Acid Centers**



## 2. THEORETICAL METHODS

On the basis of previous methodological investigations, the combination of the Hartree–Fock (HF) method and the 6-311++G(2d,2p) basis set can accurately evaluate  $^{31}\text{P}$  chemical shifts.<sup>29</sup> During the calculations, the TMP–Lewis acid adsorption structures were first optimized at the HF/6-311++G(2d,2p) level. In view of the fact that calculations based on the HF method normally yield underestimated energies for the TMP–Lewis acid complexes, the calculations of single-point energies were further refined at the MP2/6-311++G(2d,2p) level. The gauge-including atomic orbitals (GIAO) formalism<sup>30</sup> was adopted to predict  $^{31}\text{P}$  chemical shifts at the HF/6-311++G(2d,2p)

**Table 1. Experimental  $^{31}\text{P}$  NMR Chemical Shift ( $\delta^{31}\text{P}$ ) of TMP Adsorbed on Brønsted and Lewis Acid Sites of Various Solid Acid Catalysts**

catalyst	$\delta^{31}\text{P}$ (ppm)		reference	Lewis acid center
	Brønsted site	Lewis site		
$\text{Al}_2\text{O}_3$	$-3.9$	$-51$	23	Al
$\text{CHCl}_3/\text{Al}_2\text{O}_3$	$-3.5$	$-44$	10	Al
$\text{AlCl}_3/\text{Al}_2\text{O}_3$	$-3.4$	$-41; -53$	10	Al
HZSM-5	$-3.5$	$-45$	9	Al
H-beta	$-4.5$	$-32; -47$	22	Al
H-Y (calined at $700^\circ\text{C}$ )	$-4.2$	$-32; -43.5; -46.5; -50.5; -54.5; -58$	6	Al
$\text{BF}_3/\text{Al}_2\text{O}_3$	$-4$	$-26$	23	B
$\text{TiO}_2$	---	$-35$	14	Ti
$\text{SO}_4^{2-}/\text{TiO}_2$	$-4$	$-24$	14	Ti
TS zeolite	$-4.8$	$-34.2; -32$	27,28	Ti
$\text{ZrO}_2$	---	$-28; -43$	24	Zr
$\text{ZrO}_2$	---	$-42.4$	25	Zr
$\text{ZrO}_2$	---	$-30.3; -42.2; -50.1$	26	Zr
$\text{SO}_4^{2-}/\text{ZrO}_2$	$-3.8$	$-33.7; -39.7; -44.4$	25	Zr
$\text{W}/\text{ZrO}_2$	$-4$	$-35$	24	W or Zr

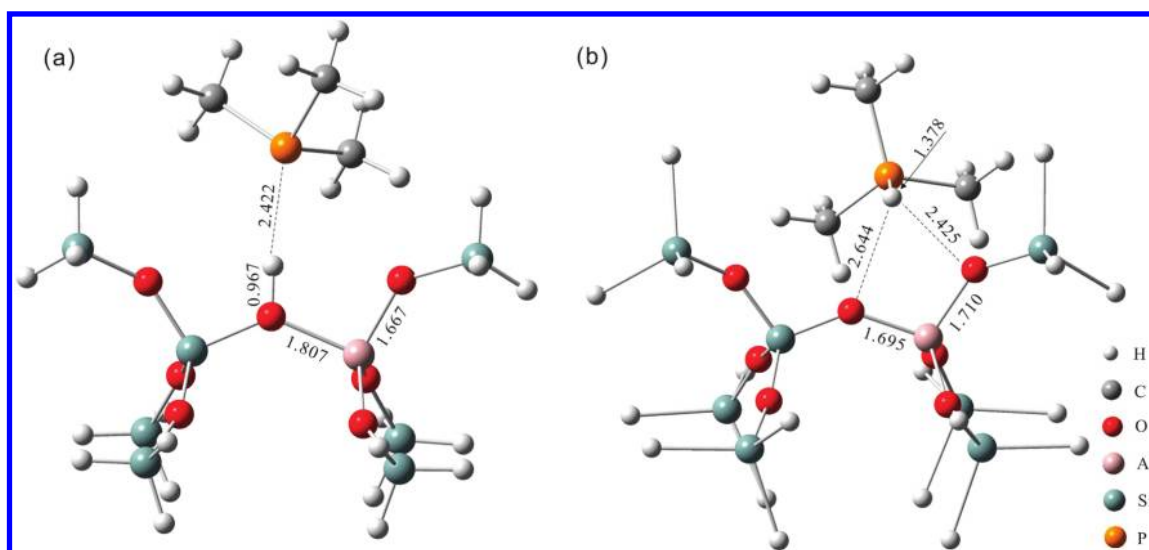


**Figure 1.** HF/6-311++G(2d,2p) optimized equilibrium configurations of (a) hydrogen-bonded and (b) protonated TMP adsorbed on the bridging hydroxyl proton (Si–OH–Al) on the 8T zeolite cluster model with a Si–H bond length of 1.20 and 2.00 Å, respectively. Selected interatomic distances (in Å) are indicated.

**Table 2.** List of Assorted  $O_z$ –H ( $r_{Oz-H}$ ) and P–H ( $r_{P-H}$ ) Bond Distances, Proton Affinities (PA), and  $^{31}\text{P}$  Chemical Shifts ( $\delta^{31}\text{P}$ ) of the Bare 8T Zeolite Cluster and TMP–Brønsted Acid Adsorption Structure with Different Si–H Bond Length from 1.10 to 2.75 Å

$r_{\text{Si-H}}$ (Å)	bare cluster		TMP adsorption structure		
	$r_{Oz-H}$ (Å)	PA (kcal/mol)	$r_{Oz-H}$ (Å)	$r_{P-H}$ (Å)	$\delta^{31}\text{P}$ (ppm)
1.10	0.944	322.8	0.965	2.441	−60
1.20	0.944	318.4	0.967	2.422	−60
1.25	0.944	316.0	2.320	1.377	−3.5
1.30	0.944	313.3	2.337	1.377	−3.5
1.50	0.945	302.4	2.408	1.377	−3.5
1.75	0.946	288.2	2.518	1.378	−3.5
2.00	0.947	274.5	2.644	1.378	−3.4
2.25	0.948	262.5	2.788	1.379	−3.2
2.50	0.949	252.2	2.784	1.378	−2.5
2.75	0.949	242.7	3.000	1.379	−1.6

level for the optimized structures. Taking the experimental  $^{31}\text{P}$  chemical shifts of gaseous TMP (−62 ppm)<sup>31</sup> as a benchmark, the calculated isotropic  $^{31}\text{P}$  NMR chemical shifts were referenced to that of liquid TMP (corresponding to a calculated absolute shift of 417 ppm). All calculations were carried out with the Gaussian09 program.<sup>32</sup>

### 3. RESULTS AND DISCUSSION

**3.1. Correlation of  $^{31}\text{P}$  Chemical Shifts of Adsorbed TMP with Brønsted Acidic Strengths.** An 8T zeolite cluster model having varied terminal Si–H bond lengths, namely,  $(\text{H}_3\text{SiO})_3\text{--Si--OH--Al--(SiOH}_3)_3$  (Figure 1), was used to represent Brønsted acid sites with different acid strengths. All terminal hydrogen atoms in the cluster were defined to locate at a distance  $r_{\text{Si-H}}$  away from the corresponding silicons during calculations, so that each Si–H bond is oriented along the direction toward

the neighboring oxygen atom. As such, Brønsted acid sites with different acidic strengths can readily be represented by varying the  $r_{\text{Si-H}}$  value in the 8T cluster model.<sup>4,19–21,33,34</sup> As shown in Table 2, upon increasing  $r_{\text{Si-H}}$  from 1.10 to 2.75 Å, the O–H bond length ( $r_{Oz-H}$ ) of the bridging hydroxyl groups gradually elongates from 0.944 to 0.949 Å.

Proton affinity (PA), defined as the energy difference between the protonated (HA) and deprotonated ( $\text{A}^-$ ) conformations (i.e.,  $\text{PA} = E_{\text{HA}} - E_{\text{A}^-}$ ), has been shown to be a suitable criterion for evaluating the intrinsic acidic strength of solid acids. A smaller PA value therefore would reflect the more ease to deprotonate a Brønsted acid (bridging hydroxyl proton) site and thus a stronger acidic strength. As shown in Table 2, upon elongating the  $r_{\text{Si-H}}$  bond length of the bare 8T cluster from 1.10 to 2.75 Å, the corresponding PA value decreases accordingly from 322.8 to 242.7 kcal/mol, covering the typical Brønsted acid strengths of solid acids from weak, medium, strong, to superacids.<sup>19,20</sup> It is noteworthy that a PA value of ca. 250 kcal/mol is considered as the threshold of super Brønsted acidity.<sup>19,33,34</sup> As such, it may be inferred that the 8T cluster model exhibits superacid property when the  $r_{\text{Si-H}}$  bond length exceeds 2.50 Å. For comparison, our additional calculations showed that bare silanol (Si–OH), which possesses an equilibrium  $r_{Oz-H}$  value of 0.938 Å, exhibited a PA value of 360.8 kcal/mol, representing a lower limit for Brønsted acidity.

Upon adsorbing trimethylphosphine (TMP), the partial negative-charged P atom on the base probe molecule tends to interact with the hydroxyl protons to form a hydrogen-bonded  $\text{TMP} \cdots \text{H}$  complex (Scheme 1b and Figure 1a) or protonated adduct ( $\text{TMPH}^+$ ; Scheme 1a and Figure 1b) depending on the acidic strength of the Brønsted acid sites. For a TMP/Brønsted acid adsorption system with  $\text{PA} \geq 318$  kcal/mol (corresponding to  $r_{\text{Si-H}} \leq 1.20$  Å; see Table 2), the formation of the hydrogen-bonded  $\text{TMP} \cdots \text{H}$  complex led to a marginal increase in  $r_{Oz-H}$  from ca. 0.944 Å (bare cluster) to 0.967 Å. Meanwhile, the distance between the P atom (of the TMP) and hydroxyl proton,  $r_{P-H}$ , slightly increases from 2.422 to 2.441 Å, while the calculated isotropic  $^{31}\text{P}$  NMR chemical shift ( $\delta^{31}\text{P}$ ) remained practically unchanged at ca. −60 ppm. These results obtained for



**Table 3.** Assorted Bond Distances between the Metallic Lewis Center and the Halogen Atoms ( $r_{M-X}$ ), Binding Energies (BE), Mulliken Charges at the P Atom ( $Q_P$ ), and  $^{31}\text{P}$  NMR Chemical Shifts ( $\delta^{31}\text{P}$ ) of TMP Adsorbed on Various Boron-, Aluminum-, and Titanium-Containing Lewis Acids and Their Mixed Halides

bare Lewis acid				TMP–Lewis acid complex			
acid center (M)	type	$r_{M-Cl}$ (Å)	$r_{M-F}$ (Å)	$r_{M-P}$ (Å)	BE (kcal/mol)	$Q_P$ ( $ e $ )	$\delta^{31}\text{P}$ (ppm)
B	$\text{BCl}_3$	1.746	---	1.986	33.51	2.63	−13
	$\text{BCl}_2\text{F}$	1.749	1.290	2.011	27.36	0.98	−22
	$\text{BClF}_2$	1.751	1.291	2.045	21.59	0.44	−30
	$\text{BF}_3$	---	1.294	2.105	16.57	0.09	−37
Al	$\text{AlCl}_3$	2.073	---	2.441	38.78	0.99	−49
	$\text{AlCl}_2\text{F}$	2.068	1.618	2.444	37.65	0.32	−51
	$\text{AlClF}_2$	2.063	1.617	2.449	36.71	0.01	−51
	$\text{AlF}_3$	---	1.615	2.454	35.96	−0.08	−52
Ti	$\text{TiCl}_4$	2.180	---	2.675	20.52	3.86	−19
	$\text{TiCl}_3\text{F}$	2.185	1.725	2.680	19.20	2.01	−25
	$\text{TiCl}_2\text{F}_2$	2.191	1.729	2.692	17.70	1.15	−32
	$\text{TiClF}_3$	2.199	1.734	2.714	16.00	0.56	−37
	$\text{TiF}_4$	---	1.738	2.755	15.37	0.18	−43

TMP adsorbed on Brønsted acid with weak acidic strengths resemble that observed for TMP/Si–OH (i.e., on bare silanol) adsorption structure, which yielded  $r_{\text{Oz-H}} = 0.946$  Å,  $r_{\text{P-H}} = 2.643$ , and  $\delta^{31}\text{P} = -62$  ppm. That the  $\delta^{31}\text{P}$  observed for the  $\text{TMP} \cdots \text{H}$  complex remains practically at ca.  $-60$  ppm for weak acid sites is consistent with experimental results.<sup>35</sup>

However, upon adsorbing TMP from weak to medium Brønsted acid sites, abrupt changes in  $r_{\text{Oz-H}}$ ,  $r_{\text{P-H}}$ , and  $\delta^{31}\text{P}$  were observed. For example, as the PA value of the bare 8T cluster changes from 318.4 to 316.0 kcal/mol, there is a sharp increase in the  $r_{\text{Oz-H}}$  bond distance from 0.967 to 2.320 Å, accompanied by a notable decrease in  $r_{\text{P-H}}$  from 2.422 to 1.377 Å as well as a drastic increase in  $\delta^{31}\text{P}$  of the  $\text{TMPH}^+$  complex from  $-60$  to  $-3.5$  ppm. Further decreasing the PA value of the bare 8T cluster from 316.0 to 262.5 kcal/mol, which corresponds to the change from medium to high Brønsted acid strength, resulted in a graduate increase in  $r_{\text{Oz-H}}$  (from 2.320 to 2.788 Å) of the  $\text{TMPH}^+$  adduct, while only slight variations in both  $r_{\text{P-H}}$  (1.377–1.379 Å) and  $\delta^{31}\text{P}$  ( $-3.5$  to  $-3.2$  ppm) were observed (Table 2). Finally, as the strength of acid sites approaches the threshold for superacidity (i.e.,  $\text{PA} \leq 250$  kcal/mol),<sup>19,29,30</sup> a further increase in  $\delta^{31}\text{P}$  beyond  $-2.5$  ppm was observed. The notable change in the  $r_{\text{Oz-H}}$  bond length from ca. 0.94–0.95 Å of the bare cluster to 2.32–3.00 Å upon adsorption of TMP onto Brønsted acid sites therefore reflected TMP in different proton environments, namely, the hydrogen-bonded  $\text{TMP} \cdots \text{H}$  complex vs the protonated  $\text{TMPH}^+$  adduct. For the latter, which is invoked by proton transfer, the density of the electron cloud surrounding the  $^{31}\text{P}$  nucleus tends to decrease with increasing acidic strength of the Brønsted acid site, which in turn causes the  $^{31}\text{P}$  resonance to shift toward a higher chemical shift (i.e., downfield direction) compared to that of gaseous TMP ( $-62$  ppm).<sup>31</sup> As such, the  $\delta^{31}\text{P}$  of the adsorbed TMP appears to be a sensitive parameter to differentiate different types of proton environments. It is noteworthy that the  $\delta^{31}\text{P}$ s of the  $\text{TMPH}^+$  adducts predicted herein at the Hartree–Fock (HF) level appear to span over a range of ca.  $-4$  to  $-2$  ppm, which is in good agreement with the available experimental  $^{31}\text{P}$  NMR results ( $-5$  to  $-3$  ppm; Table 1) obtained for various solid acids. Obviously, the stronger the acidic strength of the acid site, the larger the extent of proton transfer from the

bridging hydroxyl to TMP, which in turn leads to a slight decrease in  $r_{\text{P-H}}$  and an increase in  $\delta^{31}\text{P}$ . Nevertheless, the range of  $\delta^{31}\text{P}$  observed for the  $\text{TMPH}^+$  adduct is much narrower compared to that of  $\delta^{13}\text{C}$  of the adsorbed 2- $^{13}\text{C}$ -acetone (210–250 ppm)<sup>34</sup> or  $\delta^{31}\text{P}$  of the adsorbed trimethylphosphine oxide (TMPO; ca. 50–95 ppm),<sup>2,15–20</sup> which is much less sensitive for practical applications. Moreover, being volatile in ambient environment, the rapid motion of the  $\text{TMPH}^+$  normally gives rise to an averaged  $^{31}\text{P}$  resonance, which is unfavorable for precise determination of the distribution of Brønsted acid sites. As such, TMP may be more useful in referring to the presence of the weakly hydrogen-bonded  $\text{TMP} \cdots \text{H}$  complex (Scheme 1b) and the protonated  $\text{TMPH}^+$  adducts (Scheme 1a) rather than detailed differentiation of Brønsted acid sites with varied acidic strengths.

**3.2. Correlation of  $^{31}\text{P}$  Chemical Shifts of Adsorbed TMP with Lewis Acidic Strengths.** To explore the correlation between the  $\delta^{31}\text{P}$  of adsorbed TMP with Lewis acid strength, adducts of TMP with various boron-, aluminum-, and titanium-containing Lewis acid catalysts including those of formula  $\text{BCl}_n\text{F}_{3-n}$  ( $n = 0, 1, 2, 3$ ),  $\text{AlCl}_n\text{F}_{3-n}$  ( $n = 0, 1, 2, 3$ ),  $\text{TiCl}_n\text{F}_{4-n}$  ( $n = 0, 1, 2, 3, 4$ ), and their mixed halides (see Table 3) have been examined. Among them, aluminum trichloride ( $\text{AlCl}_3$ ) is a well-known Lewis acid catalyst for Friedel–Crafts alkylation and acylation reactions of aromatic rings,<sup>36</sup> and titanium tetrachloride ( $\text{TiCl}_4$ ) is an efficient Lewis acid catalyst for regio- and stereoselective azidolysis and iodolysis of  $\alpha,\beta$ -epoxycarboxylic acids;<sup>37</sup> whereas boron trifluoride ( $\text{BF}_3$ ) is a common Lewis acid for catalytic reactions such as isomerization and alkylation reactions.<sup>38</sup> The acidic strengths of various  $\text{BCl}_n\text{F}_{3-n}$  ( $n = 0-3$ ),  $\text{AlCl}_n\text{F}_{3-n}$  ( $n = 0-3$ ), and  $\text{TiCl}_n\text{F}_{4-n}$  ( $n = 0-4$ ) Lewis centers and their mixed halides are known to depend on the electronegativity of the group attached and may be modified by varying the Cl/F ratio of the catalysts.

The structures of the aforementioned bare B-, Al-, and Ti-containing Lewis acids and their mixed halides were first optimized (not shown) at the HF/6-311++G(2d, 2p) level. Accordingly, the bond distances between the metallic Lewis centers (B, Al, and Ti) and the halogen atoms (F, Cl) were attained, as depicted in Table 3. Likewise, the optimized structures of the TMP–Lewis

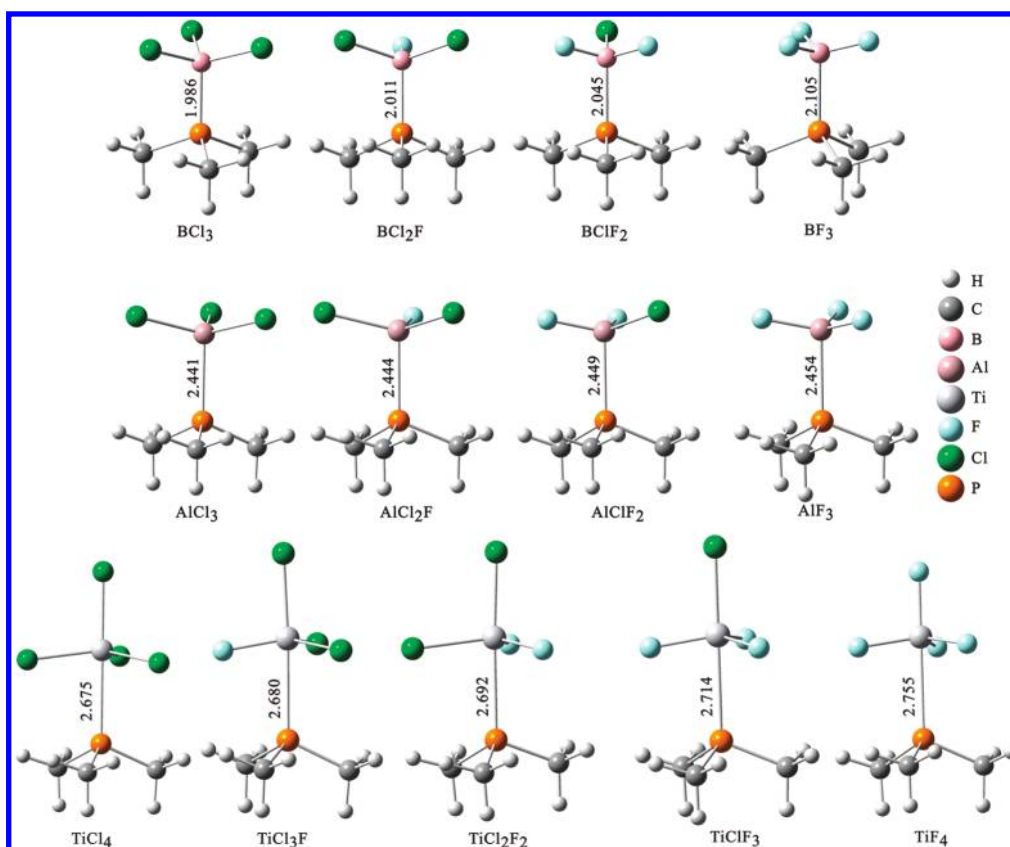


**Figure 2.** Optimized geometries of various TMP–Lewis acid complexes at the HF/6-311++G(2d,2p) level. Selective bond distances (in Å) are indicated.

acid complexes may also be obtained, as shown in Figure 2. The corresponding distances between the metallic center and P atom of the TMP probe molecule ( $r_{M-P}$ ) are listed in Table 3. Note that the B–P distance ( $r_{B-P}$ ) observed for the TMP–BCl<sub>3</sub> complex is considerably shorter than that for the TMP–BF<sub>3</sub> (1.986 vs 2.105 Å; Table 3), indicating a stronger interaction between the TMP probe molecule and the Lewis acid site in the former complex. This result is consistent with the notion that BCl<sub>3</sub> is a much stronger Lewis acid than BF<sub>3</sub>.<sup>39</sup> Likewise, similar conclusions may also be drawn for TMP–AlCl<sub>n</sub>F<sub>3–n</sub> ( $n = 0–3$ ) and TMP–TiCl<sub>n</sub>F<sub>4–n</sub> ( $n = 0–4$ ) systems. As such, it is conclusive that the Lewis acidity of B-, Al-, and Ti-containing mixed halides tends to decrease with increasing amount of F halogen atom.

It has been demonstrated<sup>40</sup> that the binding energy (BE) of some simple base probe molecules, such as NH<sub>3</sub> and CO, may be used as a theoretical measure for Lewis acidity. Utilizing NH<sub>3</sub> as the probe, Miyamoto and co-workers<sup>41</sup> have shown that the relative acid strengths follow the same trend with binding energies of Lewis acids in the order: Na<sup>+</sup> < Al(OH)<sub>2</sub><sup>+</sup> < AlO<sup>+</sup> < tricoordinated ≡ Si<sup>+</sup> in dealuminated mordenite zeolites. By the same token, we propose herein to use the BE of TMP as a measure for Lewis acidity, which may be defined as

$$BE = E_{\text{Lewis acid}} + E_{\text{TMP}} - E_{\text{TMP-Lewis acid}} \quad (1)$$

where  $E_{\text{TMP-Lewis acid}}$  represents the single-point energy of the optimized TMP–Lewis acid complex, and  $E_{\text{Lewis acid}}$  and  $E_{\text{TMP}}$  are the single-point energies of the optimized bare Lewis acid and TMP, respectively. All single-point energies were calculated at the

MP2 level using the HF method optimized geometries with the 6-311++G(2d,2p) basis set. The BE values so obtained are listed in Table 3 together with the Mulliken charges at P atom ( $Q_P$ ) and  $\delta^{31}\text{P}$ . Taking the BCl<sub>3–n</sub>F<sub>n</sub> series as an example, upon increasing the acid strength, the binding energies observed for the bare BF<sub>3</sub>, BClF<sub>2</sub>, BCl<sub>2</sub>F, and BCl<sub>3</sub> were 16.57, 21.59, 27.36, and 33.51 kcal/mol, respectively. Again, a larger BE should reflect a stronger interaction between TMP and Lewis acid site and hence a stronger Lewis acid strength. Therefore, bare BCl<sub>3</sub> is a much stronger Lewis acid than BF<sub>3</sub>, which is in good agreement with the variations of  $r_{B-P}$  observed for the TMP–BCl<sub>n</sub>F<sub>3–n</sub> ( $n = 0–3$ ) complexes. The Mulliken charges on the P atom in various TMP–Lewis complexes are also listed in Table 3. A greater  $Q_P$  value would result in a weaker shielding effect, hence shifting the <sup>31</sup>P resonance toward lower field (i.e., a larger  $\delta^{31}\text{P}$ ).<sup>42</sup> As shown in Table 3 for the TMP–BCl<sub>n</sub>F<sub>3–n</sub> ( $n = 0–3$ ) complexes, upon increasing the Lewis acid strength of the mixed halides (i.e., increasing  $n$ ), the increase in BE (16.57 to 33.51 kcal/mol) is commensurate with the increase in both  $Q_P$  (0.09 to 2.63 |e|) and  $\delta^{31}\text{P}$  (–37 to –13 ppm). The  $\delta^{31}\text{P}$  values so predicted are in good agreement with the available experimental <sup>31</sup>P NMR data. For example, for the system of BF<sub>3</sub> supported on  $\gamma$ -Al<sub>2</sub>O<sub>3</sub>, a  $\delta^{31}\text{P}$  value of –26 ppm was observed for the adsorbed TMP.<sup>23</sup> Likewise, our predicted  $\delta^{31}\text{P}$  values for TMP–AlCl<sub>n</sub>F<sub>3–n</sub> ( $n = 0–3$ ) and TMP–TiCl<sub>n</sub>F<sub>4–n</sub> ( $n = 0–4$ ) systems, which span in the range of –52 to –49 and –43 to –19 ppm with increasing  $n$ , respectively, are also in line with existing literature results obtained experimentally, e.g., for TMP adsorbed on AlCl<sub>3</sub>-modified Al<sub>2</sub>O<sub>3</sub> (–41 and –53 ppm; Table 1)<sup>10</sup> and for TMP adsorbed on TiO<sub>2</sub>

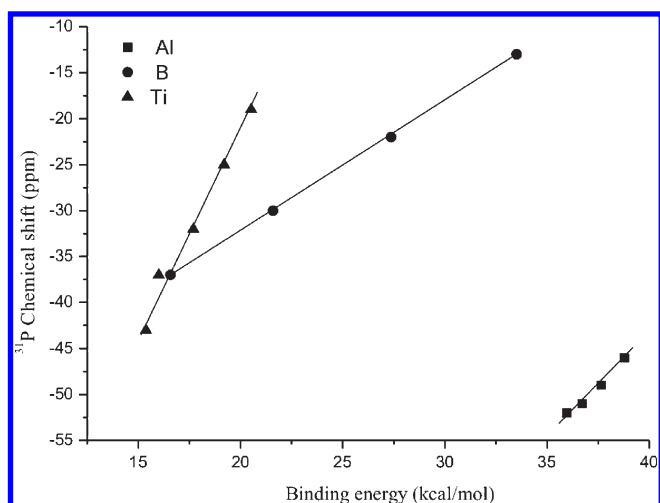


**Figure 3.** Correlations of calculated  $^{31}\text{P}$  chemical shift against binding energy of TMP adsorbed on acid sites with B-, Al-, and Ti-Lewis centers.

( $-35$  ppm),<sup>14</sup>  $\text{SO}_3/\text{TiO}_2$  ( $-24$  ppm),<sup>14</sup> and TS zeolite ( $-34.2$  and  $-32$  ppm).<sup>27,28</sup> It is noteworthy that the Mulliken charges on the P atoms are changed by ca. 1.1 |e| in the  $\text{TMP}-\text{AlCl}_{(3-x)}\text{F}_x$  complexes, while the charges are changed by ca. 2.5 and 3.7 |e| in the  $\text{TMP}-\text{BCl}_{(3-x)}\text{F}_x$  and  $\text{TMP}-\text{TiCl}_n\text{F}_{4-n}$  complexes, respectively (see Table 3). The smaller changes of the charges will result in smaller changes of the shielding around the P atoms in the  $\text{TMP}-\text{AlCl}_{(3-x)}\text{F}_x$  complexes, and thus the calculated  $^{31}\text{P}$  chemical shifts are only varied within a relatively narrow range as compared to the Ti- and B-centered Lewis acid sites.

Unlike characterization of Brønsted acidity using multinuclear solid-state NMR techniques, such as  $^1\text{H}$ ,  $^{13}\text{C}$ , and  $^{31}\text{P}$  NMR of respective pyridine, acetone, and TMPO probe molecules, which show linear correlations between the observed NMR chemical shifts and the Brønsted acidic strengths over a considerable range,<sup>2–4,15–21</sup> characterization of Lewis acidity by  $^{31}\text{P}$  NMR of adsorbed TMP appears to be somewhat less universal in terms of range of acidic strength. This may be attributed to the much simpler characteristics of Brønsted acidity in most solid acid catalysts, which typically involve bridging or terminal OH groups. As such, the strengths of these protonic acid sites may readily be correlated over a wide range with the chemical shifts observed by nuclei and corresponding probe molecules of interest. On the other hand, owing to the wide varieties of Lewis acids and the complex interactions with the base probe molecule (such as TMP) involved, a universal correlation between Lewis acid strength and physicochemical parameters (e.g., BE,  $\delta_{(31P)}$  of adsorbed TMP, etc.) is rather difficult to attain. For example, considering the empty orbitals (LUMO) of the Lewis acidity, it is anticipated that systems with a lower LUMO energy should affiliate with the base probe molecules more easily. Corma et al.,<sup>43</sup> who proposed to use the LUMO energy as a measure for Lewis acidity, emphasized that a justifiable correlation can be made only when comparing Lewis acid sites involving the same central atom (Lewis center). Moreover, the so-called hard–soft acid–base (HSAB) principle, which specifies that hard acids prefer to bind with hard bases whereas soft acids are more preferable to bind with soft bases,<sup>44</sup> also excludes the possibility of finding a universal scale for acidic strengths in Lewis acids having different metallic acid centers.

Nevertheless, we were able to obtain a linear correlation between the binding affinity (BE) and  $^{31}\text{P}$  NMR chemical shift ( $\delta_{(31P)}$ ) of TMP adsorbed on Lewis acids with B-, Al-, and Ti-acid centers individually, which may be expressed by

$$\text{BCl}_n\text{F}_{3-n} \ (n = 0-3) : \\ \delta_{(31P)} = 1.41(\pm 0.01) - 60.50(\pm 0.33) \times \text{BE}; \ R^2 = 1.00 \quad (2)$$

$$\text{AlCl}_n\text{F}_{3-n} \ (n = 0-3) : \\ \delta_{(31P)} = 2.15(\pm 0.20) - 129.64(\pm 7.46) \times \text{BE}; \ R^2 = 0.99 \quad (3)$$

$$\text{TiCl}_n\text{F}_{4-n} \ (n = 0-4) : \\ \delta_{(31P)} = 3.37(\pm 0.86) - 93.28(\pm 16.00) \times \text{BE}; \ R^2 = 0.91 \quad (4)$$

As shown in Figure 3, these empirical equations thus facilitate direct determination of Lewis acid strengths from the  $^{31}\text{P}$  chemical shift of the adsorbed TMP for a specified system having the same Lewis acid center. It is anticipated that this technique may be extended to other more complex Lewis acid systems with wide varieties of physicochemical characteristics.

## 4. CONCLUSIONS

The optimized adsorption structures of trimethylphosphine (TMP) complexed with various Brønsted and Lewis acid models with different acidic strengths have been attained theoretically at the HF/6-311++G(2d,2p) level. The corresponding  $^{31}\text{P}$  NMR chemical shifts ( $\delta_{(31P)}$ ) for these TMP–acid complexes were predicted based on the GIAO formalism.

Unlike  $^{31}\text{P}$  NMR studies using trialkylphosphine oxides ( $\text{R}_3\text{PO}$ ), by which a linear correlation between the observed  $\delta_{(31P)}$  and Brønsted acidic strength may be inferred,  $\delta_{(31P)}$  predicted for TMP adsorbed on model 8T zeolite clusters are narrower to show the specific correlation between the two parameters. Nevertheless, such study using TMP as a probe was still feasible for discernment of weakly hydrogen-bonded  $\text{TMP} \cdots \text{H}$  complexes, protonated  $\text{TMPH}^+$  adducts, and TMP–Lewis acid complexes.

In terms of characterization of Lewis acidity, while a universal correlation between the calculated  $\delta_{(31P)}$  and acid strength was not found by a similar study using  $^{31}\text{P}$  NMR of adsorbed TMP, linear correlations between  $\delta_{(31P)}$ s and binding energies of the TMP–Lewis acid complexes were, respectively, observed for  $\text{BCl}_n\text{F}_{3-n}$  ( $n = 0-3$ ),  $\text{AlCl}_n\text{F}_{3-n}$  ( $n = 0-3$ ), and  $\text{TiCl}_n\text{F}_{4-n}$  ( $n = 0-4$ ) systems over a limited range. As such, it is conclusive that TMP is not only a unique NMR probe for identifying Brønsted and Lewis acid sites present in the same solid acid catalyst but also useful for determining acid strengths of Lewis acids that comprise with the same metallic centers, for example, B-, Al-, and Ti-containing Lewis acids and their mixed halides.

## AUTHOR INFORMATION

### Corresponding Author

\*Dr. A. Zheng. E-mail: zhenganm@wipm.ac.cn. Fax: +86-27-87199291. Dr. S.-B. Liu. E-mail: sbliu@sinica.edu.tw. Fax: +886-2-23620200. Dr. F. Deng. E-mail: dengf@wipm.ac.cn. Fax: +86-27-87199291.

## ACKNOWLEDGMENT

This work was supported by the National Natural Science Foundation of China (21073228, 20933009 and 20921004) and



by the National Science Council (NSC98-2113-M-001-017-MY3), Taiwan. The authors are grateful to Shanghai Super-computer Center (SSC, China) and the National Center for High-performance Computing (NCHC, Taiwan) for their support in computing facilities.

## REFERENCES

- (1) Corma, A. Inorganic Solid Acids and Their Use in Acid-Catalyzed Hydrocarbon Reactions. *Chem. Rev.* **1995**, *95*, 559–614.
- (2) (a) Zhao, Q.; Chen, W. H.; Huang, S. J.; Wu, Y. C.; Lee, H. K.; Liu, S. B. Discernment and Quantification of Internal and External Acid Sites on Zeolites. *J. Phys. Chem. B* **2002**, *106*, 4462–4469. (b) Yu, Z.; Zheng, A.; Wang, Q.; Huang, S.; Deng, F.; Liu, S. B. Acidity Characterization of Solid Acid Catalysts by Solid-State NMR Spectroscopy: A Review on Recent Progresses. *Chin. J. Magn. Reson.* **2010**, *27*, 485–515.
- (3) Haw, J. F.; Nicholas, J. B.; Xu, T.; Beck, L. W.; Ferguson, D. B. Physical Organic Chemistry of Solid Acids: Lessons from in Situ NMR and Theoretical Chemistry. *Acc. Chem. Res.* **1996**, *29*, 259–267.
- (4) Fang, H.; Zheng, A.; Chu, Y.; Deng, F.  $^{13}\text{C}$  Chemical Shift of Adsorbed Acetone for Measuring the Acid Strength of Solid Acids: A Theoretical Calculation Study. *J. Phys. Chem. C* **2010**, *114*, 12711–12718.
- (5) Rothwell, W. P.; Shen, W.; Lunsford, J. H. Solid-State Phosphorus-31 NMR of a Chemisorbed Phosphonium Ion in HY Zeolite: Observation of Proton-Phosphorus-31 Coupling in the Solid-State. *J. Am. Chem. Soc.* **1984**, *106*, 2452–2453.
- (6) Lunsford, J. H.; Rothwell, W. P.; Shen, W. X. Acid Sites in Zeolite Y: A Solid-State NMR and Infrared Study Using Trimethylphosphine as a Probe Molecule. *J. Am. Chem. Soc.* **1985**, *107*, 1540–1547.
- (7) (a) Hunger, M. Brønsted Acid Sites in Zeolites Characterized by Multinuclear Solid-State NMR Spectroscopy. *Catal. Rev.-Sci. Eng.* **1997**, *39*, 345–393. (b) Maciel, G. E.; Ellis, P. D. In *NMR Techniques in Catalysis*; Bell, A. T.; Pines, A., Eds.; Dekker: New York, 1994; pp 231–309. (c) Hu, B.; Gay, I. D. Probing Surface Acidity by  $^{31}\text{P}$  Nuclear Magnetic Resonance Spectroscopy of Arylphosphines. *Langmuir* **1999**, *15*, 477–481.
- (8) (a) Baltusis, L.; Frye, J. S.; Maciel, G. E. Phosphorus-31 NMR Study of Trialkylphosphine Probes Adsorbed on Silica-Alumina. *J. Am. Chem. Soc.* **1987**, *109*, 40–46. (b) Chu, P. J.; Carvajal, R. R.; Lunsford, J. H. Direct NMR Spinning Sideband Analysis for a Dipolar Coupled System: Structure Elucidation of a Proton-Trimethylphosphine Complex in LaH-Y Zeolites. *Chem. Phys. Lett.* **1990**, *175*, 407–412. (c) Bendada, A.; DeRose, E.; Fripiat, J. J. Motions of Trimethylphosphine on the Surface of Acid Catalysts. *J. Phys. Chem.* **1994**, *98*, 3838–3842. (d) Sheng, T. C.; Kirszenstein, P.; Bell, T. N.; Gay, I. D.  $^{31}\text{P}$  and  $^{119}\text{Sn}$  High Resolution Solid State CP/MAS NMR Study of  $\text{Al}_2\text{O}_3\text{-SnO}_2$  Systems. *Catal. Lett.* **1994**, *23*, 119–126. (e) Haw, J. F.; Zhang, J.; Shimizu, K.; Venkatraman, T. N.; Luigi, D. P.; Song, W.; Barich, D. H.; Nicholas, J. B. NMR and Theoretical Study of Acidity Probes on Sulfated Zirconia. *J. Am. Chem. Soc.* **2000**, *122*, 12561–12570.
- (9) Zhao, B.; Pan, H.; Lunsford, J. H. Characterization of  $[(\text{CH}_3)_3\text{P-H}]^+$  Complexes in Normal H-Y, Dealuminated H-Y, and H-ZSM-5 Zeolites Using  $^{31}\text{P}$  Solid-State NMR Spectroscopy. *Langmuir* **1999**, *15*, 2761–2765.
- (10) Sang, H.; Chu, H. Y.; Lunsford, J. H. An NMR Study of Acid Sites on Chlorided Alumina Catalysts Using Trimethylphosphine as a Probe. *Catal. Lett.* **1994**, *26*, 235–246.
- (11) Kao, H. M.; Grey, C. P. Characterization of the Lewis Acid Sites in Zeolite HY with the Probe Molecule Trimethylphosphine, and  $^{31}\text{P}/^{27}\text{Al}$  Double Resonance NMR. *Chem. Phys. Lett.* **1996**, *259*, 459–464.
- (12) (a) Kao, H. M.; Grey, C. P. Determination of the  $^{31}\text{P}\text{-}^{27}\text{Al}$  J-Coupling Constant for Trimethylphosphine Bound to the Lewis Acid Site of Zeolite HY. *J. Am. Chem. Soc.* **1997**, *119*, 627–628. (b) Kao, H. M.; Grey, C. P.; Pitchumani, K.; Lakshminarasimhan, P. H.; Ramamurthy, V. Activation Conditions Play a Key Role in the Activity of Zeolite CaY: NMR and Product Studies of Brønsted Acidity. *J. Phys. Chem. A* **1998**, *102*, 5627–5638. (c) Kao, H. M.; Liu, H.; Jiang, J. C.; Lin, S. H.; Grey, C. P. Determining the Structure of Trimethylphosphine Bound to the Brønsted Acid Site in Zeolite HY: Double-Resonance NMR and Ab Initio Studies. *J. Phys. Chem. B* **2000**, *104*, 4923–4933.
- (13) Kao, H. M.; Yu, C. Y.; Yeh, M. C. Detection of the Inhomogeneity of Brønsted Acidity in H-mordenite and H- $\beta$  Zeolites: A Comparative NMR Study Using Trimethylphosphine and Trimethylphosphine Oxide as  $^{31}\text{P}$  NMR Probes. *Microporous Mesoporous Mater.* **2002**, *53*, 1–12.
- (14) Zhang, H.; Yu, H.; Zheng, A.; Li, S.; Shen, W.; Deng, F. Reactivity Enhancement of 2-Propanol Photocatalysis on  $\text{SO}_4^{2-}/\text{TiO}_2$ : Insights from Solid-State NMR Spectroscopy. *Environ. Sci. Technol.* **2008**, *42*, 5316–5321.
- (15) (a) Baltusis, L.; Frye, J. S.; Maciel, G. E. Phosphine Oxides as NMR Probes for Adsorption Sites on Surfaces. *J. Am. Chem. Soc.* **1986**, *108*, 7119–7120. (b) Osegovic, J. P.; Drago, R. S. Measurement of the Global Acidity of Solid Acids by  $^{31}\text{P}$  MAS NMR of Chemisorbed Triethylphosphine Oxide. *J. Phys. Chem. B* **2000**, *104*, 147. (c) Rakiewicz, E. F.; Peters, A. W.; Wormsbecher, R. F.; Sutovich, K. J.; Mueller, K. T. Characterization of Acid Sites in Zeolitic and Other Inorganic Systems Using Solid-State  $^{31}\text{P}$  NMR of the Probe Molecule Triethylphosphine Oxide. *J. Phys. Chem. B* **1998**, *102*, 2890–2896. (d) Karra, M. D.; Sutovich, K. J.; Mueller, K. T. NMR Characterization of Brønsted Acid Sites in Faujasitic Zeolites with Use of Perdeuterated Trimethylphosphine Oxide. *J. Am. Chem. Soc.* **2002**, *124*, 902–903.
- (16) (a) Chen, W. H.; Tsai, T. C.; Jong, S. J.; Zhao, Q.; Tsai, C. T.; Lee, H. K.; Wang, I.; Liu, S. B. Effect of Surface Modification on Coking, Deactivation and Para-Selectivity of H-ZSM-5 Zeolites during Ethylbenzene Disproportionation. *J. Mol. Catal. A* **2002**, *181*, 41–55. (b) Huang, S. J.; Tseng, Y. H.; Mou, Y.; Liu, S. B.; Huang, S. H.; Lin, C. P.; Chan, J. C. C. Spectral Editing Based on Selective Excitation and Lee-Goldburg Cross-Polarization under Magic Angle Spinning. *Solid State Nucl. Magn. Reson.* **2006**, *29*, 272–277.
- (17) (a) Zhao, Q.; Chen, W. H.; Huang, S. J.; Liu, S. B. Qualitative and Quantitative Determination of Acid Sites on Solid Acid Catalysts. *Stud. Surf. Sci. Catal.* **2003**, *145*, 205–209. (b) Chen, W. H.; Huang, S. J.; Lai, C. S.; Tsai, T. C.; Lee, H. K.; Liu, S. B. Effects of Binder, Coking and Regeneration on Acid Properties of H-mordenite during TPD Reaction. *Res. Chem. Intermed.* **2003**, *29*, 761–772. (c) Huang, S. J.; Zhao, Q.; Chen, W. H.; Han, X.; Bao, X.; Lo, P. S.; Lee, H. K.; Liu, S. B. Structure and Acidity of Mo/H-MCM-22 Catalysts Studied by NMR Spectroscopy. *Catal. Today* **2004**, *97*, 25–34. (d) Bauer, F.; Chen, W. H.; Bilz, E.; Huang, S. J.; Freyer, A.; Sauerland, V.; Liu, S. B. Surface Modification of Nano-Sized HZSM-5 and HFER by Pre-Coking and Silanization. *J. Catal.* **2007**, *251*, 258–270.
- (18) (a) Chen, W. H.; Ko, H. H.; Sakthivel, A.; Huang, S. J.; Liu, S. H.; Lo, A. Y.; Tsai, T. C.; Liu, S. B. A Solid-State NMR, FT-IR, and TPD Study on Acid Properties of Sulfated and Metal-Promoted Zirconia: Influence of Promoter and Sulfation Treatment. *Catal. Today* **2006**, *116*, 111–120. (b) Tagusagawa, C.; Takagaki, A.; Iguchi, A.; Takanabe, K.; Kondo, J. N.; Ebitani, K.; Hayashi, S.; Tatsumi, T.; Domen, K. Highly Active Mesoporous Nb-W Oxide Solid Acid Catalyst. *Angew. Chem., Int. Ed.* **2010**, *49*, 1128–1132. (c) Feng, N.; Zheng, A.; Huang, S. J.; Zhang, H.; Yu, N.; Yang, C. Y.; Liu, S. B.; Deng, F. Combined Solid-State NMR and Theoretical Calculation Studies of Brønsted Acid Properties in Anhydrous 12-Molybdophosphoric Acid. *J. Phys. Chem. C* **2010**, *114*, 15464–15472. (d) Huang, S. J.; Yang, C. Y.; Zheng, A.; Feng, N.; Wu, P. H.; Yu, N.; Chang, Y. C.; Lin, Y. C.; Deng, F.; Liu, S. B. New Insights of Keggin-type 12-Tungstophosphoric Acid from  $^{31}\text{P}$  MAS NMR of Adsorbed Trimethylphosphine Oxide and DFT Calculation Studies. *Chem. Asian J.* **2011**, *6*, 137–148.
- (19) Zheng, A.; Zhang, H.; Lu, X.; Liu, S. B.; Deng, F. Theoretical Predictions of  $^{31}\text{P}$  NMR Chemical Shift Threshold of Trimethylphosphine Oxide Adsorbed on Solid Acid Catalysts. *J. Phys. Chem. B* **2008**, *112*, 4496–4505.
- (20) Zheng, A.; Huang, S. J.; Chen, W. H.; Wu, P. H.; Zhang, H.; Lee, H. K.; De Ménorval, L. C.; Deng, F.; Liu, S. B.  $^{31}\text{P}$  Chemical Shift of



Adsorbed Trialkylphosphine Oxides for Acidity Characterization of Solid Acids Catalysts. *J. Phys. Chem. A* **2008**, *112*, 7349–7356.

(21) Zheng, A.; Zhang, H.; Chen, L.; Yue, Y.; Ye, C.; Deng, F. Relationship Between  $^1\text{H}$  Chemical Shifts of Deuterated Pyridinium Ions and Brønsted Acid Strength of Solid Acids. *J. Phys. Chem. B* **2007**, *111*, 3085–3089.

(22) Guan, J.; Li, X.; Yang, G.; Zhang, W.; Liu, X.; Han, X.; Bao, X. Interactions of Phosphorous Molecules with the Acid Sites of H-Beta Zeolite: Insights from Solid-State NMR Techniques and Theoretical Calculations. *J. Mol. Catal. A* **2009**, *310*, 113–120.

(23) Yang, J.; Zheng, A.; Zhang, M.; Luo, Q.; Yue, Y.; Ye, C.; Lu, X.; Deng, F. Brønsted and Lewis Acidity of the  $\text{BF}_3/\gamma\text{-Al}_2\text{O}_3$  Alkylation Catalyst as Revealed by Solid-State NMR Spectroscopy and DFT Quantum Chemical Calculations. *J. Phys. Chem. B* **2005**, *109*, 13124–13131.

(24) Shimizu, K.; Venkatraman, T. N.; Song, W. NMR Study of Tungstated Zirconia Catalyst: Acidic Properties of Tungstated Zirconia and Influence of Tungsten Loading. *Appl. Catal., A* **2002**, *224*, 77–87.

(25) Yu, H.; Fang, H.; Zhang, H.; Li, B.; Deng, F. Acidity of Sulfated Tin Oxide and Sulfated Zirconia: A View from Solid-State NMR Spectroscopy. *Catal. Commun.* **2009**, *10*, 920–924.

(26) Xu, J.; Zheng, A.; Yang, J.; Su, Y.; Wang, J.; Zeng, D.; Zhang, M.; Ye, C.; Deng, F. Acidity of Mesoporous  $\text{MoO}_x/\text{ZrO}_2$  and  $\text{WO}_x/\text{ZrO}_2$  Materials: A Combined Solid-State NMR and Theoretical Calculation Study. *J. Phys. Chem. B* **2006**, *110*, 10662–10671.

(27) Yang, G.; Lan, X.; Zhou, L.; Zhuang, J.; Ma, D.; Liu, X.; Han, X.; Bao, X. Acidity and Defect Sites in Tantalum Silicate Catalyst. *Appl. Catal., A* **2008**, *337*, 58–65.

(28) Zhuang, J.; Ma, D.; Yan, Z.; Deng, F.; Liu, X.; Han, X.; Bao, X.; Liu, X.; Guo, X.; Wang, X. Solid-State MAS NMR Detection of the Oxidation Center in TS-1 Zeolite by In Situ Probe Reaction. *J. Catal.* **2004**, *221*, 670–673.

(29) Zhang, Y.; Oldfield, E.  $^{31}\text{P}$  NMR Chemical Shifts in Hypervalent Oxyphosphoranes and Polymeric Orthophosphates. *J. Phys. Chem. B* **2006**, *110*, 579–586.

(30) Ditchfield, R.; Hehre, W. J.; Pople, J. A. Self-Consistent Molecular-Orbital Methods. IX. An Extended Gaussian-Type Basis for Molecular-Orbital Studies of Organic Molecules. *J. Chem. Phys.* **1972**, *54*, 724–728.

(31) Gorenstein, D. G. *Phosphorus-31 NMR: Principles and Applications*; Academic Press: Orlando, USA, 1984.

(32) Frisch, M. J. et al. *Gaussian 09*, revision A.02; Gaussian, Inc.: Pittsburgh, PA, 2010.

(33) Kramer, G. J.; van Santen, R. A.; Emeis, C. A.; Nowak, A. K. Understanding the Acid Behaviour of Zeolites from Theory and Experiment. *Nature* **1993**, *363*, 529–531.

(34) (a) Zheng, X.; Blowers, P. An Ab Initio Study of Ethane Conversion Reactions on Zeolites Using the Complete Basis Set Composite Energy Method. *J. Mol. Catal. A* **2005**, *229*, 77–85. (b) Zheng, X.; Blowers, P. Reactivity of Alkanes on Zeolites: A Computational Study of Propane Conversion Reactions. *J. Phys. Chem. A* **2005**, *109*, 10734–10741.

(35) Luo, Q.; Deng, F.; Yuan, Z.; Yang, J.; Zhang, M.; Yue, Y.; Ye, C. Using Trimethylphosphine as a Probe Molecule to Study the Acid Sites in Al-MCM-41 Materials by Solid-State NMR Spectroscopy. *J. Phys. Chem. B* **2003**, *107*, 2435–2442.

(36) (a) Sanders, S. D.; Ruiz-Olalla, A.; Johnson, J. S. Total Synthesis of (+)-Virgatusin via  $\text{AlCl}_3$ -Catalyzed  $[3 + 2]$  Cycloaddition. *Chem. Commun.* **2009**, *34*, 5135–5137. (b) Bini, L.; Pidko, E. A.; Muller, C.; van Santen, R. A.; Vogt, D. Lewis Acid-Controlled Regioselectivity in Styrene Hydrocyanation. *Chem.—Eur. J.* **2009**, *15*, 8768–8778.

(37) Fringuelli, F.; Pizzo, F.; Vaccaro, L. Lewis-Acid Catalyzed Organic Reactions in Water. The Case of  $\text{AlCl}_3$ ,  $\text{TiCl}_4$ , and  $\text{SnCl}_4$  Believed To Be Unusable in Aqueous Medium. *J. Org. Chem.* **2001**, *66*, 4719–4722.

(38) Russell, G. A. Catalysis by Metal Halides. IV. Relative Efficiencies of Friedel-Crafts Catalysts in Cyclohexane-Methylcyclopentane Isomerization, Alkylation of Benzene, and Polymerization of Styrene. *J. Am. Chem. Soc.* **1959**, *81*, 4834–4838.

(39) (a) Bess, F.; Frenking, G. Why is  $\text{BCl}_3$  a Stronger Lewis Acid with Respect to Strong Bases than  $\text{BF}_3$ ? *Inorg. Chem.* **2003**, *42*, 7990–7994.

(b) Hirao, H.; Omoto, K.; Fujimoto, H. Lewis Acidity of Boron Trihalides. *J. Phys. Chem. A* **1999**, *103*, 5807–5811. (c) Lindeman, L. P.; Wilson, M. K. Vibration Spectra of Some Mixed Halides of Boron. *J. Chem. Phys.* **1956**, *24*, 242–249.

(40) Lamberov, A. A.; Kuznetsov, A. M.; Shapnik, M. S.; Masliy, A. N.; Borisevich, S. V.; Romanova, R. G.; Egorova, S. R. Quantum-Chemical Investigation of the Formation of Lewis Acid Centers of High-Siliceous Zeolites. *J. Mol. Catal. A* **2000**, *158*, 481–486.

(41) Elanany, M.; Koyama, M.; Kubo, M.; Broclawik, E.; Miyamoto, A. Periodic Density Functional Investigation of Lewis Acid Sites in Zeolites: Relative Strength Order as Revealed from  $\text{NH}_3$  Adsorption. *App. Surf. Sci.* **2005**, *246*, 96–101.

(42) Mehring, M. *High Resolution NMR in Solids*, 2nd ed.; Springer-Verlag: New York, 1983.

(43) Corma, A.; Garcia, H. Lewis Acids: From Conventional Homogeneous to Green Homogeneous and Heterogeneous Catalysis. *Chem. Rev.* **2003**, *103*, 4307–4366.

(44) Parr, R. G.; Pearson, R. G. Absolute Hardness: Companion Parameter to Absolute Electronegativity. *J. Am. Chem. Soc.* **1983**, *105*, 7512–7516.